Journal of Power Sources 206 (2012) 490–496

Contents lists available at ScienceDirect

Journal of Power Sources

journal homepage: www.elsevier.com/locate/jpowsour

Degradation mechanisms in the non-aqueous vanadium acetylacetonate redox flow battery☆

Aaron A. Shinkle[a], Alice E.S. Sleightholme[a], Lucas D. Griffith[a], Levi T. Thompson[a,b], Charles W. Monroe[a,*]

[a] Department of Chemical Engineering, University of Michigan, Ann Arbor 48109-2136, USA
[b] Department of Mechanical Engineering, University of Michigan, Ann Arbor 48109-2136, USA

ARTICLE INFO

Article history:
Received 9 September 2010
Received in revised form 8 December 2010
Accepted 22 December 2010
Available online 14 January 2011

Keywords:
Vanadium acetylacetonate
Single-metal redox flow battery
Non-aqueous electrolyte
Organic electrochemistry
Energy-storage

ABSTRACT

Electrochemical and physical measurements elucidate several thermodynamic properties and chemical factors that affect the performance of a non-aqueous all-vanadium flow battery. An H-type test cell was constructed that demonstrates stable coulombic efficiencies of 70% without flow after several weeks of slow cycling, with a steady plateau voltage near 1.7 V during most of the discharge step. Environmental oxygen and water are associated with side reactions that affect long-term charge/discharge response of the battery. Oxygen passivates the electrode and may react with the solvent or supporting electrolyte, while water can cause the formation of oxovanadium complexes. Reversible cycling of the vanadyl acetylacetonate complex appears possible.

1. Introduction

Grid penetration of intermittent renewable energy sources, which is presently increasing at rates of up to 50% per annum [1], cannot continue without a parallel development of methods to store massive quantities of energy. Redox flow battery (RFB) systems promise efficient, scalable energy storage well suited for such large-scale applications [2,3]. Interest in flow batteries began more than 30 years ago and several system chemistries have been demonstrated in the intervening decades [2,3]. The most commonly implemented systems sustain little capacity fade over time, are minimally susceptible to self-discharge, and have relatively high energy and power efficiencies. Existing RFB technologies are used to manage excess capacity on the utility grid [4] and level or shave the intermittent power delivered by distributed wind or solar energy systems [5,6].

Fundamental performance characteristics of an RFB cell are determined primarily by the redox-active species, solvent, supporting electrolyte, and separator material. The choice of redox-active species determines the RFB cell voltage. In combination with the solvent, the active species also dictate the electrochemical stability and charge capacity of the fluids. Separator materials inhibit RFB self-discharge. Because ions from the supporting electrolyte move across the separator to maintain an overall charge balance during cell operation, the separator and support also affect the power and energy efficiency of the battery [7]. State-of-the-art RFB systems offer saturated active-species concentrations of 2–3 M [8]. When tested in H-cell configurations they yield coulombic efficiencies of 75–85% and discharge at potentials near 1.5 V with energy efficiencies of 60–70% [9,10]; more refined reactor designs demonstrate coulombic efficiencies of up to 97% with 86% energy efficiency [11]. Most RFBs use water as a solvent, an acid support, and a microporous [7] or ion-exchange membrane [12] separator.

The original RFB configurations used different redox-active species in the anolyte (which contains the negative electrode, an anode during discharge) and catholyte (positive, a cathode during discharge). Examples of dual-active-species RFB chemistries include the iron/chromium, iron/titanium, and sodium-polysulfide/bromine hybrid systems, as well as the recently commercialized zinc/bromine hybrid system [13–17]. Like polymer-electrolyte fuel cells, all RFB implementations suffer from active-species crossover, and most require periodic electrolyte reactivation following long-term operation [7,18,19]. Dual active-species chemistries may be problematic because they can degrade irreversibly when constituents of the anolyte and catholyte mix.

☆ This paper is based on work presented at the International Flow Battery Forum, 15; 16 June 2010. The aim of the International Flow Battery Forum is to encourage the discussion and dissemination of information relating to the research, development, demonstration, manufacture and operation of flow battery components and systems.

* Corresponding author. Tel.: +1 734 647 4645; fax: +1 734 763 0459.
E-mail address: cwmonroe@umich.edu (C.W. Monroe).

0378-7753/$ – see front matter © 2011 Elsevier B.V. All rights reserved.
doi:10.1016/j.jpowsour.2010.12.096

Single active-metal RFBs, which include the popular aqueous all-vanadium system suggested by Pelligri and Spaziante [20] and later realized by Skyllas-Kazacos [21–23], mitigate the crossover problem by employing redox-active species that contain a single active-metal center. In single-metal RFBs, crossover only causes self-discharge, a reversible process that can occur without degrading the electrolyte materials.

Although it relies on a single active metal, the aqueous all-vanadium system employs four distinct redox-active species to maintain a sufficiently high cell voltage. During discharge, V^{V} reduces to V^{IV} on the positive electrode and V^{II} oxidizes to V^{III} at the negative electrode. The catholyte contains vanadyl and pervanadyl ions, whereas the anolyte contains vanadium ions. In sulfuric acid at pH near zero, the all-vanadium RFB half-reactions are [22–26]

$$VO_2^+ + 2H^+ + e^- \leftrightarrow VO^{2+} + H_2O \quad E^\theta = 1.000\,V \text{ vs. SHE}, \tag{1}$$

$$V^{3+} + e^- \leftrightarrow V^{2+} \quad E^\theta = 0.291\,V \text{ vs. SHE}, \tag{2}$$

Thus the overall cell reaction is

$$V^{2+} + VO_2^+ + 2H^+ \leftrightarrow V^{3+} + VO^{2+} + H_2O \quad \Delta E^\theta = -1.291\,V. \tag{3}$$

The support acid provides protons, making the equilibrium cell potential pH-dependent. Crossover in single-metal RFBs has been observed to cause as much as 10% self-discharge over 72 h [27]. Since this self-discharge involves the mixing of various oxovanadium ions with vanadium ions, the anolyte and catholyte in the aqueous all-vanadium RFB may still require periodic regeneration during the lifetime of the battery. Also, half-reaction (1) is kinetically sluggish due to the high reorganization energy of the oxovanadium species.

Chemistries that exploit one- or two-electron disproportionation of chargeable metal complexes [28–31] further refine the single-metal RFB concept because they minimize the need for regeneration steps. Recently Liu et al. [32] reported that vanadium acetylacetonate, $V(acac)_3$, could be used as the active material for a single-metal RFB involving only three redox-active species. It was proposed that the dominant electrochemical half-reactions in the non-aqueous vanadium acetylacetonate RFB are

$$V(acac)_3^+ + e^- \leftrightarrow V(acac)_3, \tag{4}$$

and

$$V(acac)_3 + e^- \leftrightarrow V(acac)_3^-. \tag{5}$$

During discharge, V^{IV} reduces to V^{III} according to reaction (4) on the positive electrode and V^{II} oxidizes to V^{III} on the negative electrode. The overall reaction is

$$V(acac)_3^+ + V(acac)_3^- \leftrightarrow 2V(acac)_3. \tag{6}$$

If crossover of either charged complex occurs, the negatively and positively charged species will combine in the solution phase, causing self-discharge by formation of the neutral intermediate. No regeneration is required. Since support ions are not involved in reaction (6), the concentration of supporting electrolyte should not affect the equilibrium voltage.

Only three adjacent oxidation states of vanadium appear in reaction (6), as opposed to the four states in reaction (3). Yet the energetics of half-reactions (4) and (5) lead to a standard cell potential near 2.2 V for the $V(acac)_3$ RFB reaction (6) – ~0.8 V higher than reaction (3) in 2 M H_2SO_4. Using non-aqueous supporting electrolytes, the $V(acac)_3$ RFB system has been operated for many cycles without significant deterioration [32].

This paper presents a further study of the non-aqueous vanadium acetylacetonate RFB chemistry. The discussion emphasizes how the use of non-aqueous RFB chemistries requires consideration of several new engineering aspects. For instance, the exposure of system materials to environmental oxygen and water before and during battery assembly can significantly affect performance. The charge/discharge response over long-term cycling is discussed in light of these environmental effects.

2. Experimental

2.1. Solution preparation

Non-aqueous electrolytic solutions consisted of anhydrous acetonitrile (CH_3CN, 99.8%, Aldrich, U.S.) solvent with tetraethylammonium tetrafluoroborate ($TEABF_4$, 99%, Fluka, U.S.) supporting electrolyte. Vanadium(III) acetylacetonate ($V(acac)_3$, 97%, Aldrich, U.S.) or vanadyl(II) acetylacetonate ($VO(acac)_2$, 98%, Aldrich, U.S.) active metal species were used for non-aqueous voltammetry. For solubility studies, binary solutions of $V(acac)_3$ in anhydrous CH_3CN were prepared. Charge/discharge experiments were performed with anolyte and catholyte comprised of $V(acac)_3$ and $TEABF_4$ in CH_3CN. Aqueous electrolytic solutions were prepared by dissolving vanadium(IV) oxide sulfate hydrate ($VOSO_4{\cdot}xH_2O$, 99.99%, Alfa Aesar, U.S.) and sulfuric acid (99.999%, Aldrich, U.S.) in deionized water (18 MΩ, Millipore Milli-Q Advantage).

2.2. Cyclic voltammetry

Cyclic voltammetry was performed in an airtight three-compartment cell using an Autolab PGSTAT302N Potentiostat/Galvanostat (Ecochemie, Netherlands). In all voltammetry experiments, the working electrodes were 3 mm diameter (0.07 cm^2 area) glassy-carbon disk electrodes (Basi, U.S.), which were polished with 15, 6, and 0.1 μm silicon carbide polishing paper, washed, and dried for 8 h prior to each experiment. The counterelectrode was a 5 cm^2 graphite plate (Graphite Store, U.S.), which was cleaned with 15 μm silicon carbide polishing paper, sonicated for 15 min, and dried for 8 h prior to each experiment.

Reference electrodes were connected to the working-electrode compartment of the electrochemical cell via a Luggin capillary. A saturated mercury/mercurous sulfate (Radiometer Analytical, France) reference electrode was used for measurements with the aqueous electrolytic solution. Voltammetry of the non-aqueous solutions was performed using an Ag/Ag^+ (Basi, U.S.) reference electrode, which consisted of a silver-metal electrode immersed in a solution of 0.01 M silver nitrate (Basi, U.S., 99%) and 0.1 M tetraethylammonium perchlorate (Alfa Aesar, U.S., 98%). A bridging solution of 0.05 M tetraethylammonium nitrate (Fluka, U.S., 98%) was used to establish a thermodynamically meaningful potential for working electrodes immersed in the $TEABF_4$ support.

All the solutions were deoxygenated with pre-purified nitrogen (99.998%) prior to experiments, which were performed under a blanket of flowing nitrogen unless stated otherwise. For experiments involving oxygen, solutions were subsequently oxygenated with oxygen gas (99.993%). All the presented results were obtained after performing several cycles at 500 mV s^{-1} (until the voltammogram stabilized – typically 15 cycles) to remove any residual electrochemically active contaminants.

2.3. Battery cycling

Charge/discharge tests in a glass H-type cell were performed using an experimental design essentially similar to the test reported by Liu et al. [32]. The H-cell used for the present study was smaller, however, with an interelectrode distance of approximately 9 cm, a membrane area of 2 cm^2, and anolyte and catholyte solutions with 10 mL volumes. A Neosepta AHA anion-exchange membrane (ASTOM, Japan) was used to separate the anolyte and catholyte. Prior to cell assembly, the membrane was soaked in

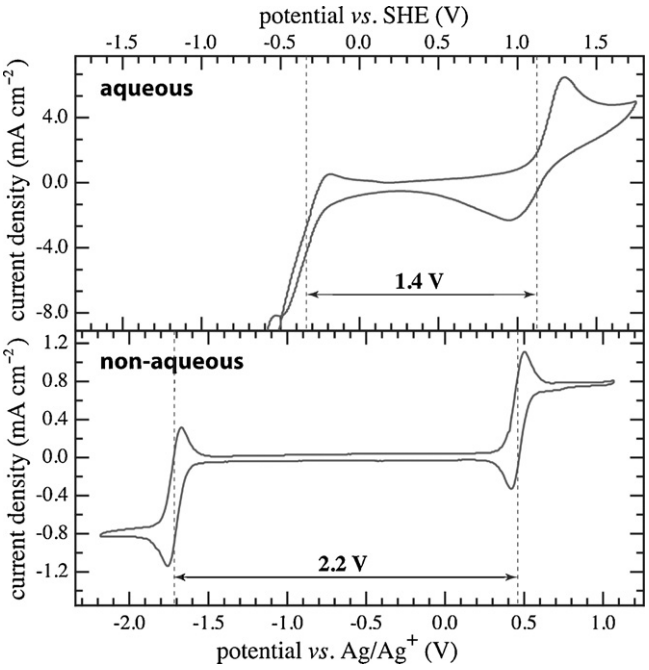

Fig. 1. Comparison of cyclic voltammograms with a glassy carbon disk electrode in (aqueous) 0.01 M $VOSO_4$ and 2 M H_2SO_4 in ultrapure H_2O and (non-aqueous) 0.01 M $V(acac)_3$ and 0.1 M $TEABF_4$ in CH_3CN. Scan rate 10 mV s^{-1}; measurements performed at room temperature.

the test solution for more than 24 h. The H-cell was assembled, filled with liquids, and cycled in an argon-atmosphere glove box (MBraun, U.S.) to prevent contamination by ambient air.

Both the positive and negative electrodes were graphite plates (The Graphite Store, U.S., P/N BL001230), which were polished with 15 μm silicon carbide paper, sonicated for 15 min, and dried for 8 h prior to the experiment. At the beginning of the experiment the electrodes were partially immersed to depths such that each liquid/electrode contact area was 7 cm^2.

The charge/discharge study was performed using anolyte and catholyte solutions comprising 0.05 M $V(acac)_3$ and 0.5 M $TEABF_4$ in CH_3CN. During cycling, both sides of the H-cell were continuously stirred with Teflon-coated stir bars. The arms of the H-cell were capped to prevent solvent evaporation, which was insignificant over the several-week duration of the experiment.

Electric currents were controlled using a Maccor Series 4000 48-channel battery tester (Maccor, U.S.). Changes in the voltage response were observed during 11 cycles of galvanostatic charge and discharge. Discharge steps were performed at 0.014 mA cm^{-2} until a state of full discharge (a cell potential at or below 0.1 V) was reached. Charge steps were performed at 0.14 mA cm^{-2} from full discharge up to 50% of the theoretical maximum state of charge (SOC). Thus charge steps were performed at a nominal C/14 rate based on the theoretical maximum catholyte SOC, while discharge steps were performed at a nominal C/140 rate.

3. Results and discussion

3.1. Comparison of aqueous and non-aqueous all-vanadium systems

Fig. 1 shows two cyclic voltammograms, of 0.01 M $VOSO_4$ in 2 M aqueous sulfuric acid and 0.01 M $V(acac)_3$ supported by 0.1 M $TEABF_4$ in acetonitrile. As has been reported elsewhere, the aqueous system affords a cell potential of ~1.4 V [22–24,33], although the equilibrium potential associated with the negative couple is difficult to distinguish because of the large current associated with hydrogen evolution at low voltages.

No significant features arising from electrochemical side reactions appear in the non-aqueous voltammogram in Fig. 1. Two significant redox couples are visible, which can be associated with single-electron oxidation or reduction of the $V(acac)_3$ complex [32]. The mean separation of the anodic and cathodic peaks in the non-aqueous voltammogram yields a formal potential of $E = 0.46$ V vs. Ag/Ag$^+$ for reaction (4), and of $E = -1.72$ V for reaction (5).

The 1.4 V cell potential for the aqueous system is somewhat higher than the 1.29 V predicted by the standard potentials of the aqueous V^{II}/V^{III} and V^{IV}/V^{V} couples. This difference arises because the reduction potential of reaction (1) changes with pH [33]. No similar effect needs be considered in the non-aqueous system. Because supporting ions are not involved in half-reactions (4) or (5), the cell potential of the non-aqueous $V(acac)_3$ RFB is unaffected by support concentration. Thus the 2.18 V equilibrium cell potential observed here agrees with the potential reported by Liu et al. [32], despite the fact that those experiments were performed with a fivefold higher $TEABF_4$ concentration.

From a system engineering perspective, it is significant that no aspect of the support structure is dictated by the non-aqueous RFB cell reaction. Thus both the cation and the anion comprising the supporting electrolyte can in principle be varied without altering the battery's fundamental electrochemistry. Several non-aqueous electrolytes dissociate in CH_3CN and are electrochemically inert over the potential window between −1.72 and 0.46 V vs. Ag/Ag$^+$ [34]. Although $TEABF_4$ is very electrochemically stable, various alternatives could be chosen to optimize the ionic conductivities (to increase power efficiency of the RFB reactor) or lower the volumetric costs of the anolyte and catholyte.

The maximum volumetric charge capacities of the anolyte and catholyte, which are determined by the solubilities of the redox-active species, are fundamental performance metrics of any RFB chemistry. But the solubilities of organometallic active species for RFBs cannot be measured very easily because those complexes tend to absorb light in the visible spectrum. Very concentrated solutions are nearly opaque, making it difficult to measure solubility by standard techniques.

To estimate the solubility of $V(acac)_3$ in CH_3CN without direct observation of precipitates, a set of density measurements was utilized. If density ρ varies linearly with solute concentration c, then the partial molar volume $\bar{V}$ of the solute is constant [35] and a plot of solution density vs. solute concentration can be used to compute

$$\bar{V} = \frac{M - (\partial\rho/\partial c)_{T,p}}{\rho_0}, \tag{7}$$

where M is the molar mass of solute and ρ_0 is the solvent density. The concentration of a saturated solution, c_{sat}, can be estimated from its density ρ_{sat} through

$$c_{sat} = \frac{\rho_{sat} - \rho_0}{M - \rho_0\bar{V}}. \tag{8}$$

Fig. 2 illustrates the densities of binary solutions of $V(acac)_3$ in CH_3CN as a function of the $V(acac)_3$ molar concentration. Within the 1% experimental error, the density varied linearly with respect to concentration of the solute. When incorporated into Eq. (7), the slope of the linear fit in Fig. 2 yields $\bar{V} = 256$ mL mol^{-1} for $V(acac)_3$ in CH_3CN. A saturated solution of $V(acac)_3$ was observed to have a density of 0.865 g mL^{-1}. Based on Eq. (8), the saturated concentration of $V(acac)_3$ in CH_3CN is 0.59 ± 0.02 M at room temperature (~23 ± 1 °C).

Aqueous vanadyl sulfate has a solubility of 3 M in pure water, falling to 2 M in a 2 M sulfuric-acid support [8]. Given the measurement above, the practically obtainable maximum concentration of $V(acac)_3$ in CH_3CN is approximately one-third that of vanadium in the aqueous system. Taking its larger cell potential into account, the $V(acac)_3$ in CH_3CN system should have a maximum volumetric

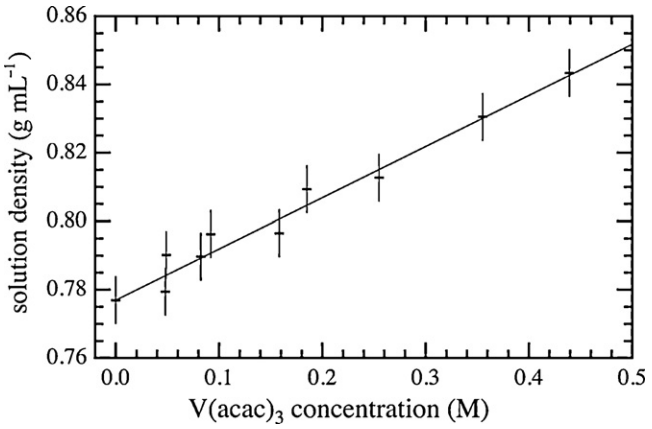

Fig. 2. Densities of binary solutions of vanadium acetylacetonate in acetonitrile as a function of solute concentration. The points represent experimental measurements and the line is a linear fit ($R^2 = 0.97$) forced through the density of pure CH_3CN at room temperature.

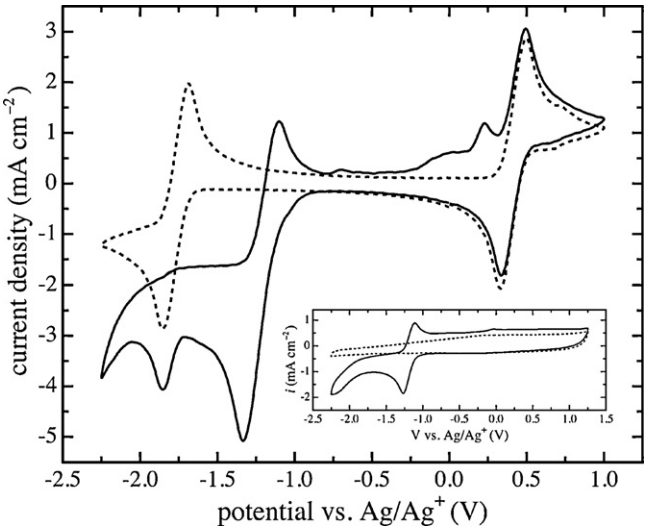

Fig. 3. Comparisons of cyclic voltammograms with a glassy carbon electrode in deoxygenated (dotted line) and oxygenated (solid line) solutions of 0.01 M V(acac)$_3$ and 0.05 M $TEABF_4$ in CH_3CN. Scan rate 100 mV s^{-1}; measurements performed at room temperature. Inset: cyclic voltammograms at 200 mV s^{-1} of a similar system without active species present.

energy density approximately two-thirds that of aqueous $VOSO_4$ in H_2O. While the energy density for this non-aqueous vanadium chemistry is lower than the aqueous chemistry, the effective power and energy efficiencies of a non-aqueous battery stack may be comparable because of the advantageous mechanical properties of acetonitrile. At ambient temperature the density of CH_3CN is three-quarters that of water and its viscosity, about a third as large. Parasitic power and energy losses owing to pumping loads could, in principle, be two-thirds lower for non-aqueous RFBs.

One should also bear in mind that acetylacetonate is just one member of a broad class of beta-diketonate ligands. Functionalization or alteration of ligand structure could be used to change solubility limits [36], and may also have an effect on cell potential [30,37]. For instance, experiments using the method described in this section show that V(acac)$_3$ has much higher solubility in CH_3CN than vanadyl acetylacetonate, which precipitates at concentrations above 0.06 M. Further studies in this area are underway.

3.2. Environmental effects

Regardless of the solvent or active species in an RFB, side reactions that consume the active metal can significantly reduce charge storage capacity. To maintain reproducible, constant charge capacity over many cycles, flow-battery assembly procedures should be designed to prevent all irreversible reactions involving the active metals. Both oxygen and water may act as environmental impurities that cause degradation of non-aqueous RFB systems. Several experiments were performed to assess whether oxygen or water adversely affect the non-aqueous V(acac)$_3$ RFB chemistry.

Fig. 3 compares cyclic voltammograms of deoxygenated and oxygenated solutions of V(acac)$_3$ in $TEABF_4$-supported CH_3CN. After 2 min of bubbling with oxygen gas, several features appear, which persist for many cycles. The presence of dissolved molecular oxygen brings about a step to a very negative limiting current at low voltages, as well as manifesting a reversible redox couple near −1.25 V vs. Ag/Ag$^+$ and several irregular oxidation features over the range between 0.0 and 0.5 V vs. Ag/Ag$^+$. The oxidation peak associated with the V(acac)$_3$/V(acac)$_3^-$ couple appears to be suppressed almost entirely by oxygen, and the reduction peak is smaller. Note that the formation of oxygen-functionalized groups on carbon electrode surfaces has been shown to impede aqueous RFB reactions [23].

Generally the negative limiting current is associated with oxygen reduction. Nawi has associated irregular peaks ranging over 0.5 V below the V(acac)$_3$ oxidation couple to acetylacetonate oxidation [38]. The redox couple at −1.25 V vs. Ag/Ag$^+$ remains visible when cyclic voltammetry is performed using an oxygenated support solution in the absence of V(acac)$_3$, however (see inset in Fig. 3), suggesting that the associated reactions do not involve the active species. When the oxygenated solution was purged of O_2 by bubbling with N_2 for 15 min, the deoxygenated voltammetric signature was reproduced identically. These observations suggest that any irreversible degradation of the active species by oxygen (associated with the peaks between 0 and 0.5 V vs. Ag/Ag$^+$) was minimal, and that the largest voltammetric features brought about by O_2 arise from reactions involving the carbon electrode surface, the solvent, or the supporting electrolyte.

Water can have a more pernicious effect than oxygen on vanadium complexes. The V^{III} center is particularly sensitive to oxidation, easily forming a VO double bond (and producing free H^+) when exposed to water [39] – a reaction also observed in the aqueous all-vanadium system [21]. In non-aqueous solvents, V(acac)$_3$ is susceptible to the ligand-substitution half-reaction [40]

$$V(acac)_3 + H_2O \leftrightarrow VO(acac)_2 + Hacac + H^+ + e^-, \quad (9)$$

where water is consumed to form vanadyl acetylacetonate (VO(acac)$_2$) and molecular acetylacetone (Hacac, a protonated acetylacetonate ion).

To test sensitivity of the system constituents to environmental water, an experiment was performed in which liquid H_2O was added to the $TEABF_4$-supported V(acac)$_3$ solution in CH_3CN. Fig. 4 compares the voltammograms obtained from the water-free solution and the hydrated solution. Note that the voltammetry of the hydrated solution did not stabilize with respect to cycle number. The data reported are for the third cycle after the addition of water; all the observed features shown in the figure continued to increase somewhat in magnitude, but additional features did not appear with continued cycling during the 1-h timeframe of the experiment.

Upon adding water to the non-aqueous vanadium acetylacetonate RFB electrolyte, small oxidation peaks form near −1.0 and 0.25 V vs. Ag/Ag$^+$. These features are consistent with oxidation of the vanadium center via reaction (9), which has been hypothesized to proceed by a two-step mechanism [38] consisting of oxidation via reaction (4) followed by an irreversible step:

$$V(acac)_3^+ + H_2O \rightarrow VO(acac)_2 + Hacac + H^+. \quad (10)$$

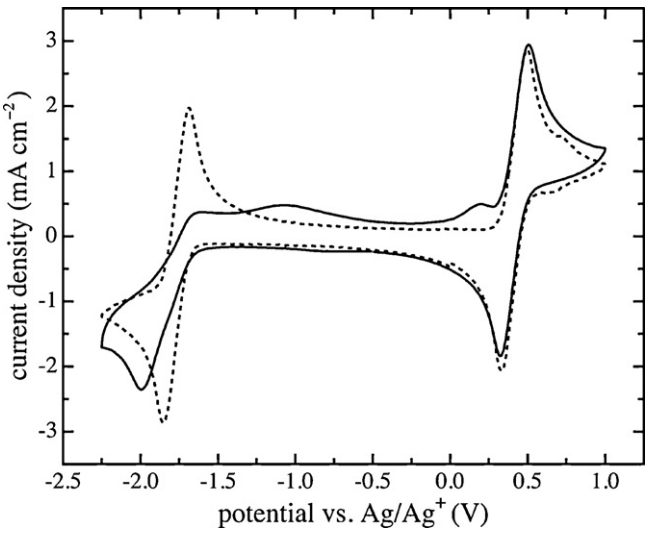

Fig. 4. Comparisons of cyclic voltammograms with a glassy carbon electrode for water-free (dotted line) and hydrated (solid line) solutions of 0.01 M V(acac)$_3$ and 0.05 M TEABF$_4$ in CH$_3$CN. Scan rate 100 mV s^{-1}; measurements performed at room temperature. The hydrated experiment contains 4 vol% water.

Since reaction (10) is non-electrochemical, the formal potential of reaction (9) is indistinguishable from that of reaction (4). The peak in the voltammogram at 0.25 V vs. Ag/Ag$^+$, however, can be attributed to the oxidation of free acac$^-$ anions, while the broad oxidation peak near −1.0 V vs. Ag/Ag$^+$ appears similar to one observed elsewhere when Hacac was added to supported non-aqueous V(acac)$_3$ solutions [38]. Although peaks corresponding to products of reaction (10) were observed, peaks corresponding to redox activity of the VO(acac)$_2$ complex were not. This could owe to the time-frame of the experiment, which was too short for appreciable VO(acac)$_2$ to form.

Dissolved H$_2$O significantly affects the negative vanadium couple (reaction (5)). The reduction peak shifts to more negative potential and the oxidation wave takes on a sigmoidal shape, with the oxidation peak disappearing almost entirely. Water thus appears to impede the kinetics of V(acac)$_3$ reduction in both the anodic and cathodic directions. During the operation of a flow battery the presence of dissolved water could therefore induce significant increases in kinetic overpotential on the negative electrode during charge and discharge steps.

Once formed, VO(acac)$_2$ must be taken to very negative voltages (below −2.0 V) in an Hacac enriched solution to reform V(acac)$_3$ [38,41]. Thus VO(acac)$_2$ is expected to remain in the RFB system after it appears. It is unclear whether the conversion of V(acac)$_3$ to VO(acac)$_2$ impedes overall function of the RFB. Fig. 5 compares cyclic voltammograms of V(acac)$_3$ and VO(acac)$_2$ active species in similar non-aqueous supporting electrolytes. In previous work regarding the non-aqueous vanadium RFB chemistry, a redox couple at ~0.75 V vs. Ag/Ag$^+$ has been observed and attributed to a V^{IV}/V^{V} couple [32]. This couple could arise from VO(acac)$_2$ formed electrochemically in the presence of dissolved water, which cycles in the battery according to the half-reaction

$$VO(acac)_2^+ + e^- \leftrightarrow VO(acac)_2. \quad (11)$$

Fig. 5 suggests that this reaction is kinetically quasi-reversible. (It is difficult to draw conclusions about coulombic reversibility from peak-height ratios, because the peaks are superimposed on an upward step in current arising from a mass-transfer limitation.) A couple which can be associated with VO(acac)$_2$ reduction to VO(acac)$_2^-$ according to

$$VO(acac)_2 + e^- \leftrightarrow VO(acac)_2^-, \quad (12)$$

is also visible at ~−2.0 V vs. Ag/Ag$^+$.

The formation of VO(acac)$_2$ during battery cycling could lead to a mixed potential on the positive and negative electrodes associated with reactions (11) and (12), respectively. This would make the non-aqueous system operate comparably to the aqueous system, in the sense that the charge/discharge response of the system would reflect the redox behavior of four or more redox-active complexes.

In air one would expect reaction (9) to occur in parallel with the reduction of molecular oxygen, leading to the overall reaction

$$4V(acac)_3 + 2H_2O + O_2 \leftrightarrow 4VO(acac)_2 + 4Hacac. \quad (13)$$

A free-energy calculation leads to the expectation that reaction (9) will occur on the positive RFB electrode if reaction (13) goes spontaneously to completion in ambient air – *i.e.*, if the reduction potential of Eq. (9) is less than the reduction potential of O$_2$.

The progression of reaction 13 was investigated by studying the redox activity of the solid V(acac)$_3$ precursor as it aged in air over time. Fig. 5 shows a voltammogram of a solution prepared using a V(acac)$_3$ solid precursor that had been aged for several months in ambient air. Peaks corresponding to V(acac)$_3$ oxidation and reduction (half-reactions (4) and (5)) and VO(acac)$_2$ oxidation and reduction (reactions (11) and (12)) are apparent in the voltammogram, providing clear evidence that VO(acac)$_2$ forms from V(acac)$_3$ in air. Moreover, the peak heights associated with V(acac)$_3$ have decreased in height by almost half, suggesting that reaction (13) has been driven to a significant extent toward completion. An oxidation peak at 0.25 V vs. Ag/Ag$^+$ is also visible, suggesting the presence of acetylacetone derivatives.

To ensure that cell reaction (6) occurs in the non-aqueous vanadium acetylacetonate RFB, it is crucial to eliminate ambient water and air, and to take care that the precursors used to prepare anolyte and catholyte solutions are not exposed to air.

3.3. Charge/discharge tests

Charge/discharge characteristics for an H-type cell containing 0.05 M V(acac)$_3$ and 0.5 M TEABF$_4$ in CH$_3$CN were evaluated. Special care was taken to eliminate molecular oxygen from the system, and fresh 97% purity V(acac)$_3$ and 99.8% anhydrous acetonitrile were used to construct the cell in an Ar-atmosphere glove box. Cycling was performed at very low rates, with a total of 11 cycles performed

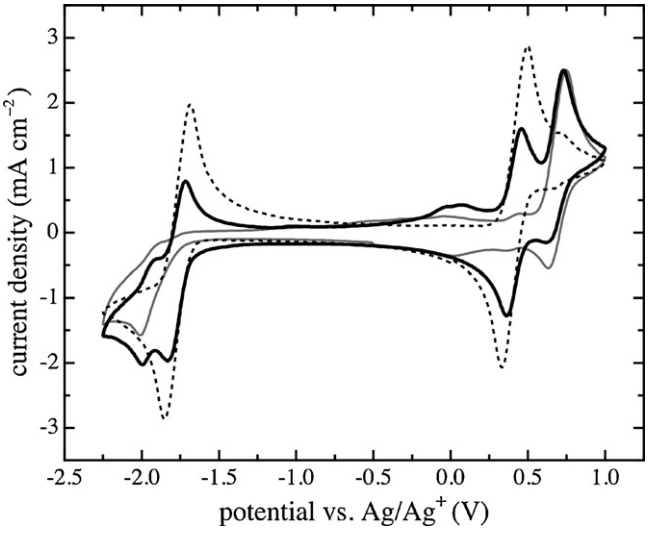

Fig. 5. Comparison of cyclic voltammograms with a glassy carbon electrode for 0.01 M V(acac)$_3$ and 0.05 M TEABF$_4$ in CH$_3$CN (dotted line), 'aged' 0.01 M V(acac)$_3$ and 0.05 M TEABF$_4$ in CH$_3$CN (black line), and 0.01 M VO(acac)$_2$ and 0.05 M TEABF$_4$ in CH$_3$CN (grey line). Scan rate 100 mV s^{-1}; measurements performed at room temperature.

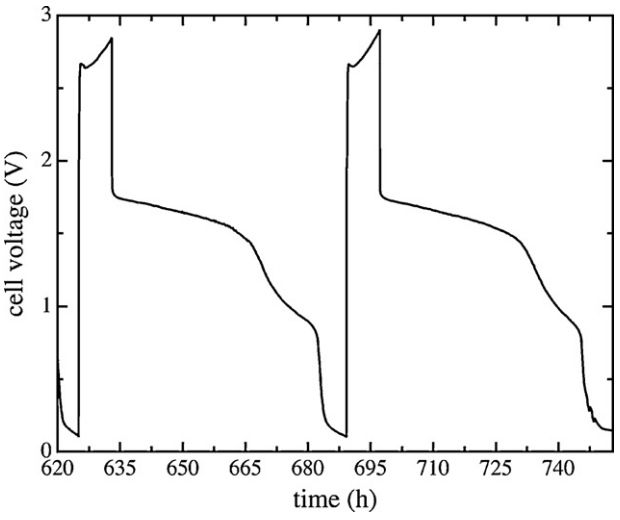

Fig. 6. Charge/discharge response during the 10th and 11th cycles of 0.05 M $V(acac)_3$ and 0.5 M $TEABF_4$ in CH_3CN in an H-cell with graphite electrodes and a Neosepta AHA separator. Charge current density 0.14 mA cm^{-2}, discharge current density 0.014 mA cm^{-2}. Measurements performed at room temperature in an Ar-atmosphere glove box.

over a period of several weeks. The nominal charge rate was C/14 based on the theoretical maximum SOC assuming one-electron disproportionation of $V(acac)_3$, and the nominal discharge rate was C/140. Charge steps were run from 0 to 50% of the theoretical maximum SOC, and discharge steps ran back down to 0% SOC.

The voltage at end-of-charge increased gradually and discharge characteristics changed over the first few cycles. Coulombic and energy efficiencies rose gradually until the fifth cycle, after which stable, qualitatively similar charge/discharge curves were achieved. Fig. 6 illustrates cycles 10 and 11.

Charge and discharge voltages are respectively higher and lower than the formal cell potential established by voltammetry. Ohmic overpotentials in the solutions arise from the low conductivity of the electrolyte and the relatively large distance between the two electrodes in the H-cell. Using an equivalent conductance obtained from 0.1 M $TEABF_4$ in CH_3CN [34] to compute the conductivity of the 0.05 M support solution, the ohmic resistance of the liquid phases was found to be approximately 160 Ω. This suggests that the H-cell configuration led to overpotentials of approximately 200 mV across the liquids during charge and 20 mV during discharge. Note that the solution resistances are a rectifiable source of energy-efficiency loss arising from the stagnant H-cell configuration used for the charge/discharge experiments in this study. Ohmic overpotentials across the liquid phases can be eliminated almost entirely in practice by employing a flow-through reactor with high-surface-area electrodes. Calculations based on independent measurements of the solution, membrane, and kinetic resistances show that the solutions and membrane account for more than 90% of the overpotential in the H-cell. Removal of the solution resistances would lead to an energy-efficiency increase of 25% over the values reported in this work.

After solution resistances are eliminated, the ionic resistance of the membrane separator is the primary source of overpotential losses. To develop more efficient non-aqueous RFB designs, ongoing investigations should focus on membrane materials. The Neosepta AHA anion-exchange membrane used here was selected for its stability in contact with the acetonitrile solvent, and may not be optimal for non-aqueous RFB scale-up. Preliminary electrochemical impedance spectroscopy studies suggest a membrane resistance of approximately 350 Ω cm^2 in conditions similar to those used for the charge/discharge experiments reported here.

Several factors must be considered when selecting membranes for non-aqueous RFB systems, and these criteria differ from those that pertain to aqueous chemistries. The aqueous all-vanadium RFB reaction, for instance, involves H^+ ions and uses an acidic supporting electrolyte, making proton-exchange membranes a logical choice. Non-aqueous solvents tend to be aprotic, and either degrade or inhibit the ion conduction of many standard proton-exchange membranes. Detailed further study should focus on determining what membranes are stable in and wet by non-aqueous solvents, what membranes resist active-species crossover, and which supporting ions provide the highest mobilities.

Charge voltages reached ~2.8 V for the two cycles shown, suggesting a total overpotential of 500–600 mV with respect to the 2.2 V formal potential associated with reaction (6). Two discharge plateaus appeared at ~1.7 V and ~1.0 V. The plateau at 1.7 V is also consistent with a 500–600 mV overpotential with respect to reaction (6). The second plateau at 1.0 V may have been associated with byproducts of the vanadyl formation reaction. Assuming an overpotential of 500 mV, a 1.5 V potential would be consistent with $acac^-$ oxidation on the positive electrode of the battery accompanied by $V(acac)_3$ reduction on the negative electrode.

Coulombic efficiencies of ~70–73% were measured for cycles 10 and 11, which are similar to those obtained in early aqueous all-vanadium experiments using H-cells [10] and 20% lower than state-of-the-art [11]. The second discharge plateau has been attributed to byproducts of $VO(acac)_2$ formation, but since the vanadyl species appears to be cyclable, its formation should not be associated with significant coulombic efficiency loss. Due to the long time-scale of the experiment, a 30% coulombic efficiency loss could owe in part to crossover of the active species through the separator, either by diffusion or by migration. (Both cationic and anionic complexes are formed from the neutral $V(acac)_3$ upon charging. Therefore, migration of the $V(acac)_3^-$ species across the anion-exchange separator is expected.) Energy efficiencies of 34% were achieved for the two cycles shown, which could potentially be enhanced by altering the system geometry or increasing electrode surface areas to reduce kinetic overpotentials (as mentioned earlier, the energy efficiency would rise to ~60% if solution resistances alone were eliminated). Since kinetic overpotentials associated with cycling of the $VO(acac)_2$ complex appear to be larger than those associated with $V(acac)_3$, formation of the vanadyl complex could adversely affect energy efficiency. A flow-through reactor with high-surface-area electrodes would be expected to reduce these kinetic losses.

Even when the cell is cycled under an inert argon atmosphere with a $V(acac)_3$ precursor that has never contacted air, residual environmental contaminants from the supporting electrolyte, membrane, or electrodes can lead to side reactions that degrade the active material. Fig. 7 presents a cyclic voltammogram of the catholyte after the charge/discharge experiment shown in Fig. 6 had run to completion. Peaks in the CV can be rationalized by the experimental results discussed above. The step downward in current which begins below −1.25 V could be associated with reduction of a dissolved component, possibly dissolved oxygen; peaks at −2.0 V and 0.75 V are associated with oxidation and reduction of the vanadyl acetylacetonate complex, as shown in Fig. 5. It is likely that the $VO(acac)_2$ forms via reaction (9), consuming residual components during the first few charge/discharge cycles before cycling efficiencies stabilize. Peaks associated with oxidation of the acetylacetonate ligand near −0.5 V vs. Ag/Ag^+ are visible, and are consistent with the ligand-shedding mechanism proposed by Nawi and Riechel [38].

The coulombic efficiencies and energy efficiencies measured here exceed those reported in earlier tests using a similar cell geometry [32] by 50% and 500%, respectively. The dramatic increase in energy efficiency could owe in part to the use of a Neosepta

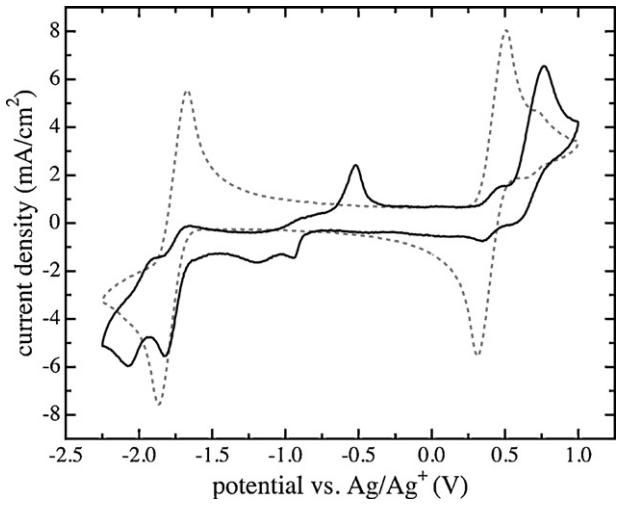

Fig. 7. Cyclic voltammograms of the catholyte before (dotted line) and after (solid line) performing the charge/discharge experiment presented in Fig. 6. Ar atmosphere; glassy carbon electrode; scan rate 500 mV s^{-1}; room temperature. Pure acetonitrile was used to dilute the V(acac)$_3$ concentration down to 0.0125 M before voltammetry was performed.

AHA anion-exchange membrane instead of AMI-7001. Also, kinetic overpotentials could have been significantly higher in the earlier experiments if appreciable amounts of VO(acac)$_2$ were present in the active-metal precursor. Studies are underway to quantify how the electrode kinetics and separator material impact the observed overpotentials.

4. Summary

Performance characteristics of the non-aqueous vanadium acetylacetonate RFB were evaluated. The 2.18 V cell potential [32] was shown to be relatively independent of supporting-electrolyte concentration. The impact of oxygen and water on cyclic voltammetry of the system were studied. Oxygen was shown to block the reduction of V(acac)$_3$ on carbon and may degrade the solvent and support. Vanadyl acetylacetonate was observed to form in the presence of water, either spontaneously in ambient air or electrochemically at the positive electrode. Water was also shown to impede kinetics of the negative V(acac)$_3$ redox couple. The VO(acac)$_2$ species was associated with positive and negative redox couples centered at ~0.75 and −2.0 V vs. Ag/Ag$^+$.

Charge/discharge characteristics of the system were assessed using an H-cell with an anion-exchange membrane separator. Two discharge plateaus were observed at approximately 1.7 V and 1.0 V. The plateau at 1.7 V is associated with the single-electron disproportionation of V(acac)$_3$, whereas the plateau at 1.0 V may owe to byproducts arising from formation of vanadyl complexes. Coulombic and energy efficiencies of ~70% and ~35%, respectively, were obtained when charging from 0% to 50% of theoretical maximum SOC for the tenth and eleventh cycles. Both efficiencies were higher than those obtained previously [32]. The increases owed in part to the use of a different anion-exchange membrane, but were probably also enhanced by the exclusion of ambient air during cell assembly.

The non-aqueous vanadium acetylacetonate redox flow battery chemistry offers a higher formal potential than the aqueous all-vanadium RFB and uses fewer redox-active species, minimizing the need for electrolyte regeneration. The solubility of vanadium acetylacetonate in acetonitrile is ~0.6 M at room temperature. Further studies to increase the solubility of the active vanadium species are ongoing.

Acknowledgments

The authors acknowledge financial support from the Advanced Energy for Transportation Technology Program and the Hydrogen Energy Technology Laboratory. The authors would also like to thank Kurt Kurzenhauser and Colleen Xinyi Wang for their valuable assistance with impedance and solubility measurements.

References

[1] Energy Information Administration, Renewable Energy Annual 2007, U.S. Department of Energy (DOE/EIA), 2009, April.
[2] M. Bartolozzi, Journal of Power Sources 27 (3) (1989) 219–234.
[3] C.P. de Leon, A. Frias-Ferrer, J. Gonzalez-Garcia, D.A. Szanto, F.C. Walsh, Journal of Power Sources 160 (1) (2006) 716–732.
[4] P. Lex, B Jonshagen, Power Engineering Journal 13 (3) (1999) 142–148.
[5] T.E. Lipman, R. Ramos, D.M. Kammen, An Assessment of Battery and Hydrogen Energy Storage Systems Integrated with Wind Energy Resources in California, PIER Final Project Report, 2005.
[6] D.C. Holzman, Environmental Health Perspectives 115 (7) (2007) A358–A361.
[7] P. Arora, Z.M. Zhang, Chemical Reviews 104 (10) (2004) 4419–4462.
[8] F. Rahman, M. Skyllas-Kazacos, Journal of Power Sources 72 (2) (1998) 105–110.
[9] P.J. Hall, E.J. Bain, Energy Policy 36 (12) (2008) 4352–4355.
[10] I. Tsuda, K. Nozaki, K. Sakuta, K. Kurokawa, Solar Energy Materials and Solar Cells 47 (1-4) (1997) 101–107.
[11] M. Kazacos, M. Skyllas-Kazacos, Journal of the Electrochemical Society 136 (9) (1989) 2759–2760.
[12] T. Sukkar, M. Skyllas-Kazacos, Journal of Membrane Science 222 (1-2) (2003) 235–247.
[13] H.S. Lim, A.M. Lackner, R.C. Knechtli, Journal of the Electrochemical Society 124 (8) (1977) 1154–1157.
[14] P.M. O'Donnell, R.F. Gahn, J.L. Pfeiffer, The Redox Flow System for Solar Photovoltaic Energy Storage, Lewis Research Center, 1976, NASA TM 73562.
[15] R.F. Savinell, C.C. Liu, R.T. Galasco, S.H. Chiang, J.F. Coetzee, Journal of the Electrochemical Society 126 (3) (1979) 357–360.
[16] P. Zhao, H.M. Zhang, H.T. Zhou, B.L. Yi, Electrochimica Acta 51 (6) (2005) 1091–1098.
[17] S.H. Ge, B.L. Yi, H.M. Zhang, Journal of Applied Electrochemistry 34 (2) (2004) 181–185.
[18] R.A. Assink, Journal of Membrane Science 17 (2) (1984) 205–217.
[19] E. Wiedemann, A. Heintz, R.N. Lichtenthaler, Journal of Membrane Science 141 (2) (1998) 215–221.
[20] A. Pelligri, P.M. Spaziante, Process and accumulator for storing and releasing electrical energy, Patent GB 2030349 A, United Kingdom (1980).
[21] M. Skyllas-Kazacos, M. Rychcik, R.G. Robins, A.G. Fane, M.A. Green, Journal of the Electrochemical Society 133 (5) (1986) 1057–1058.
[22] E. Sum, M. Rychcik, M. Skyllas-Kazacos, Journal of Power Sources 16 (2) (1985) 85–95.
[23] E. Sum, M. Skyllas-Kazacos, Journal of Power Sources 15 (2-3) (1985) 179–190.
[24] G. Oriji, Y. Katayama, T. Miura, Electrochimica Acta 49 (19) (2004) 3091–3095.
[25] J.O. Hill, I.G. Worsley, L.G. Hepler, Chemical Reviews 71 (1) (1971) 127–137.
[26] G. Oriji, Y. Katayama, T. Miura, Journal of Power Sources 139 (1-2) (2005) 321–324.
[27] M. Rychcik, M. Skyllas-Kazacos, Journal of Power Sources 19 (1) (1987) 45–54.
[28] Y. Matsuda, K. Tanaka, M. Okada, Y. Takasu, M. Morita, T. Matsumurainoue, Journal of Applied Electrochemistry 18 (6) (1988) 909–914.
[29] Y. Shiokawa, H. Yamana, H. Moriyama, Journal of Nuclear Science and Technology 37 (3) (2000) 253–256.
[30] T. Yamamura, Y. Shiokawa, H. Yamana, H. Moriyama, Electrochimica Acta 48 (1) (2002) 43–50.
[31] C.H. Bae, E.P.L. Roberts, R.A.W. Dryfe, Electrochimica Acta 48 (3) (2002) 279–287.
[32] Q.H. Liu, A.E.S. Sleightholme, A.A. Shinkle, Y.D. Li, L.T. Thompson, Electrochemistry Communications 11 (12) (2009) 2312–2315.
[33] M. Gattrell, J. Park, B. MacDougall, J. Apte, S. McCarthy, C.W. Wu, Journal of the Electrochemical Society 151 (1) (2004) A123–A130.
[34] C.G. Zoski (Ed.), Handbook of Electrochemistry, Elsevier, Amsterdam, 2007.
[35] J. Newman, K. Thomas-Alyea, Electrochemical Systems, 3 ed., John Wiley & Sons, Hoboken, NJ, 2004.
[36] G.M. Mamardashvili, N.Z. Mamardashvili, O.A. Golubchicov, B.D. Berezin, Journal of Molecular Liquids 91 (1–3) (2001) 189–191.
[37] C. Tsiamis, C.C. Hadjikostas, S. Karageorgiou, G. Manoussakis, Inorganica Chimica Acta 143 (1) (1988) 17–23.
[38] M.A. Nawi, T.L. Riechel, Inorganic Chemistry 20 (7) (1981) 1974–1978.
[39] F.A. Cotton, G. Wilkinson, Advanced Inorganic Chemistry, in: 5th ed., John Wiley & Sons, New York, 1988.
[40] M. Kitamura, K. Yamashita, H. Imai, Bulletin of the Chemical Society of Japan 49 (1) (1976) 97–100.
[41] M.A. Nawi, T.L. Riechel, Inorganic Chemistry 21 (6) (1982) 2268–2271.